Lawrence Berkeley National Laboratory
Lawrence Berkeley National Laboratory

Title
High Current Ion Sources and Injectors for Heavy Ion Fusion

Permalink
https://escholarship.org/uc/item/24v6t0tn

Author
Kwan, Joe W.

Publication Date
2005-02-15

eScholarship.org Powered by the California Digital Library
University of California

High Current Ion Sources and Injectors for Heavy Ion Fusion

Joe W. Kwan
Lawrence Berkeley National Laboratory,
1 cyclotron Road, Berkeley, California, 94720 USA

Abstract

Heavy ion beam driven inertial fusion requires short ion beam pulses with high current and high brightness. Depending on the beam current and the number of beams in the driver system, the injector can use a large diameter surface ionization source or merge an array of small beamlets from a plasma source. In this paper, we review the scaling laws that govern the injector design and the various ion source options including the contact ionizer, the aluminosilicate source, the multicusp plasma source, and the MEVVA source.

1. Introduction

The concept of heavy ion beam driven inertial fusion, commonly called heavy ion fusion (HIF), is to use ion beams to deliver high intensity pulsed power to a small D-T target. In order to have a small focal spot, the emittance must be low. Thus the research goal in developing ion sources and injectors for HIF is to produce high current ion beams with high brightness. The choice of ions is not very important as long as it has the right mass.

For a typical 5-mm diameter target, the required beam energy is about 3–7 MJ to be delivered within a pulse length of 10 ns [1]. When applying pulsed power to a fusion target, the energy must be deposited near the surface layer in order to achieve implosion. This desirable penetration range is 0.02 to 0.2 g/cm^2 of the target material. For heavy ions with atomic mass near 200, the allowable kinetic energy is <10 GeV. At this beam energy, the required beam charge is about 1 mC. Lighter ions need less kinetic energy but more current (or charge) in order to deliver the same power.

If the beam pulse length is 10 ns, it takes 100 kA to deliver 1 mC of charge. Traditional accelerators can produce high current by using storage rings, but this method is viewed as being too costly. The other approach, which is adopted by the USA, is to use induction linacs [2]. These two approaches have very different requirements on the ion sources. For storage rings, the beam charge can be accumulated using traditional low current, long pulse sources; whereas ion sources for induction linacs are required to produce high current in short pulses.

An induction linac can compress the ion beam during acceleration. For example, a pulse length of ~10,000 ns at the injector can be reduced to ~300 ns by the end of the accelerator and then further drift compressed to ~10 ns by the time it reaches the target. The starting beam current at the ion source is about 50 – 100 A (more for lighter ions). In order to keep the space charge problem (associated with high current heavy ion beams) under control, a full HIF driver system is envisioned to contain an array of ~100 parallel ion beam channels at ~0.5 A each. Even at this level, the HIF injector is characterized by its properties of simultaneously high current and high brightness.

Theoretically, the beam brightness is proportional to J/T, where J is the current density and T is the effective ion temperature. High brightness demands either high current density and/or low ion temperature. High average current density also results in small beam line cross-section and therefore minimizes the size of the induction cores.

Although heavy ions with mass >100 are ultimately needed for fusion drivers, lighter ions such as K^+ and Ar^+ are useful because they allow experiments at low energy during the early development phases. High charge state ions are desirable if they can be made without mixing several charge states together.

Energy spread results in chromatic aberration at the final focusing lens system. Large energy spread also limits the longitudinal beam compression for achieving high current. One common origin of energy spread is due to resonance charge exchange occurring in the region just outside the ion source aperture where the gas pressure is significant. Thus HIF sources require low pressure.

Table 1 shows the typical parameters of a HIF injector. These numbers may vary depending on the actual ion mass, charge state and other system design parameters. Some numbers such as the charge state purity, current profile uniformity and energy spread are simply today's best guesses and have not been fully analyzed.

Table 1: HIF driver ion source and injector specifications

Parameter	Value
Beam energy (MeV)	1.6–2.0
Beam current per beam channel (A)	0.5
Beam pulse width (μs)	20
Beam rise-time (fraction of pulse width)	≤ 5%
Repetition rate (Hz)	10
Ion mass (amu)	84–238
Charge state purity	> 90%
Emittance (π mm.mrad, normalized, 4rms)	< 1.0
Current fluctuation and variation	≤ 1%
Current profile uniformity	> 95%
Beam energy spread (kV)	≤ 2
Lifetime (pulses)	10^8

2. Beam Extraction and Transport Physics

The options for ion sources are closely coupled to the beam transport limitations in the injector. In this section, we briefly discuss the scaling laws

governing the transport physics. All electrostatic devices are governed by the "three-halves scaling law" [3]:

$$J \propto \frac{V^{3/2}}{L^2} \tag{1}$$

where J is the current density, V is the applied voltage, and L is the characteristic length of the system. The most common place to apply this scaling law is in space charge limited flow regions where the current is self-adjusting, e.g., in an extraction diode. If the dimensions are fixed and all the voltages applied to the electrodes (including the initial kinetic energy of the charged particles) increase by the same factor k, then the particle trajectories remain identical as long as the current density is increased by the factor $k^{3/2}$. The current will also increase by the same factor as the current density. The time of flight is decreased by the factor $k^{1/2}$.

In another situation, if all the voltages in the system are fixed but the dimension is increased by a factor d, then the particle trajectories remain similar as long as the current density is decreased by the factor d^2. The current, which is the product of current density and area, remains unchanged. The time of flight is increased by the factor d.

The two factors can be combined by varying both the dimension and the voltage together (in order to avoid breakdown). Usually when applying the scaling law, the current remains space charge limited, and the ion kinetic energy is proportional to beam voltage. The ions' thermal energy and contact potential at the emitting surface are usually ignored if they are much smaller than the extraction voltage.

The maximum value of V that can be applied to a device is limited by voltage breakdown, so an important rule to consider here is how the breakdown threshold scales with dimension [3,4]. For a 1 cm gap, the typical maximum operating voltage is about 100 kV. For gaps shorter than 1.0 cm, V scales linearly with distance, whereas for larger gaps >> 1 cm, typical of HIF applications, V is approximately proportional to the square root of distance. In either case, and according to Eq. (1), we find the current density decreases with increasing size. The nonlinear relationship is especially unfavorable to high current systems that require very high voltages and therefore need very large gaps.

The extraction diode can be approximated as a plane parallel space-charge-limited flow. Its current density is governed by the Child-Langmuir relationship:

$$J = \chi \frac{V^{3/2}}{d^2} \tag{2}$$

where $\chi = (4\varepsilon_o/9)(2q/M)^{1/2}$ is called the Child-Langmuir constant, with q and M being the charge and mass of the ions respectively, d is the effective extractor gap length, and V is the extraction voltage. This equation is a special form of Eq. (1).

For a circular aperture with radius a, and ignoring any curvature of the emitting surface, the extracted beam current is given by

$$I_{CL} = \pi\chi\left(\frac{a}{d}\right)^2 V^{3/2} \tag{3}$$

The aspect ratio (a/d) is an important geometric parameter affecting the beam optics. Typically, the aspect ratio is kept to less than 0.5 in order to prevent spherical aberration at the beam edge, so the maximum beam current of a diode with good

optics is determined only by the extraction voltage and does not directly depend on the actual diode size. In practice, the beam current increases with diode size because a larger diode can withstand higher extraction voltage, but as mentioned above the current density decreases with size.

Following the extraction diode is the low energy beam transport (LEBT) section. In a typical ion gun and Einzel lens, the current density also decreases with increasing size. Furthermore, their focusing capability diminishes as the beam gains velocity. Thus at sufficiently high beam energy, e.g. > 1 MeV, quadrupole focusing will be used for high current beam systems; this is the case for heavy ion fusion drivers. For electrostatic quadrupole (ESQ) channel, the maximum transportable beam current can be written as [6]:

$$J \approx \chi \left(\frac{\Delta V_q}{b} \right) \frac{\sqrt{\Phi}}{b} \tag{4}$$

where ΔV_q is the voltage across the quadrupole electrodes, Φ is the beam energy, and b is the bore radius. Here, the ESQ focusing capability increases with beam velocity (with corresponding increase in the lattice period), thus making it an effective beam transport device at medium beam energy.

3. HIF Injector Designs

As mentioned in the introduction, the HIF driver system contains a large array of parallel ion beam channels (N ≈ 100) with each channel carrying about 0.5 A of beam current. For an ion mass of 100, the space-charge potential of this beam

is equivalent to that of a 5.0 A proton beam. So far, the traditional approach for single-beam HIF experiments is to use a large diameter surface ionization source that is capable of producing current > 0.5 A (without requiring combining beams). However, we are currently developing a new gas plasma source system to replace the surface source. We will discuss both types of ion sources in the following sections.

Examples of other applications that have larger beam current are the deuterium neutral beam injectors used in tokamaks (magnetic fusion devices) and the xenon ion propulsion systems used in spacecraft. In both cases, a plasma ion source is fitted with an extraction grid containing multiple small apertures to form a large number of beamlets. The beamlets are allowed to merge into a single beam upon leaving the accelerator. While the beam current can be large in such systems, the brightness is limited by two factors. First, the average current density of the system is much lower than that of an individual beamlet (by the factor of grid transparency) and second, the merging process will cause emittance growth. In order to overcome these disadvantages, the individual beamlets must start with very high brightness.

From a system point of view, the optimum choice of an ion source is the one that will result in a cost-effective injector. At about a few hundred mA and considering only a single beam, a large surface ionization source is the preferred choice for HIF. However for much higher current or when considering a large number of beam channels, the method of merging high current density beamlets is

preferred because it has a higher average current density and consequently allows a more compact injector design.

3.1 The Large Diameter Source Approach

Figure 1 shows the computer simulation of a 1.6 MV ion gun with 0.5 A K^+ current. Since the beam size at the ion gun exit is much larger than that required in the ESQ channel in the induction linac, an ESQ matching section is needed. A preliminary design of an 84-beam injector system based on the large diameter source approach was reported by Kwan et al [7]. The array of beams was arranged in such a way that neighboring beams could share common ESQ electrodes. However, due to the fact that the ESQ array had a much smaller foot-print than that of the injector, the design adopted a funnel shape to match the difference in size at both ends. Beams in the matching section are gradually compressed to smaller radii and also must be steered towards the axis using long ESQ channels. Figure 2 is a schematic diagram of the outer-most beam line in the array.

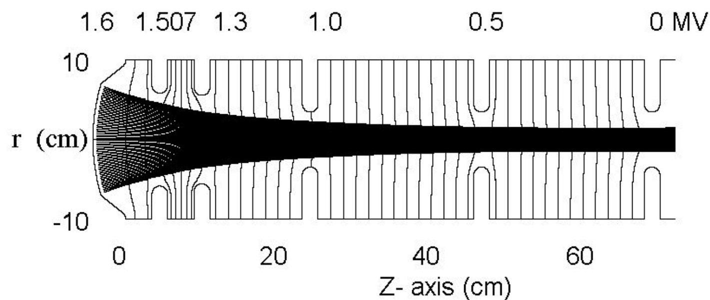

Fig. 1. Simulation of a 1.6 MV, 0.5 A ion gun with a 14 cm diameter K^+ surface ionization source.

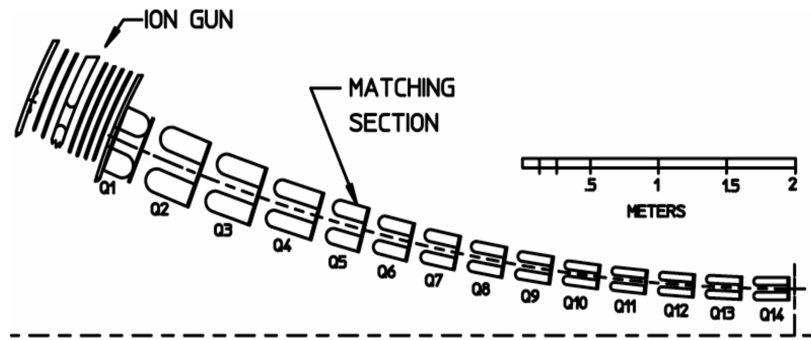

Fig. 2. Schematic diagram of the outermost beam line in an 84-beam array injector using large diameter surface ionization sources.

The main issues with this design are due to the complexity caused by beam steering and the large size. For a given electric field, the stored energy increases linearly with electrode size, therefore the very large size raises concerns in high voltage breakdown damage. For most electrode material, the stored energy that can cause damage during a voltage breakdown is a few joules. For safety, large electrodes must be kept at a lower voltage gradient. Naturally cost also increases with size as well. In considering the development path for HIF, it is clear that a more compact injector design is needed.

3.2 The Merging Multi-Beamlets Approach

In the merging multi-beamlets approach, the high current density beamlets are kept separated from each other by the acceleration grids. After pre-acceleration to reduce the charge density, the beamlets are merged together to form a high current beam (e.g., > 0.5 A). The final beam brightness depends on the emittance of

the merged beam. Figure 3 is a schematic diagram of an injector based on this concept. The total length from the ion source exit to the end of the merging/matching section is about 1.0 m. With a high enough average current density, the injector's transverse dimension can match that of the ESQ channel, so the system is not funnel-shaped. Comparing the two approaches (Fig 2 and 3), we find that the merging beamlet method can be up to six times smaller in size [8].

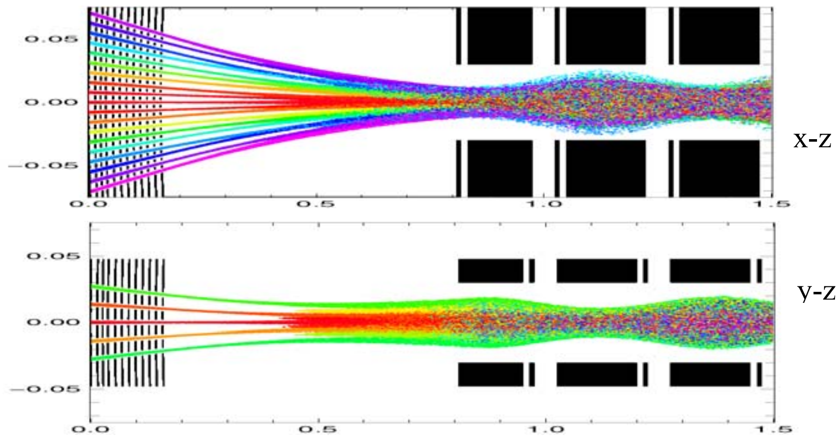

Fig. 3. Conceptual injector design based on merging a large number of beamlets.

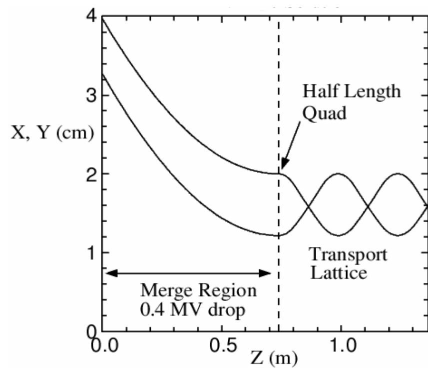

Fig.4. Beam envelopes in x-z and y-z planes showing an elliptical arrangement of beamlets allows the merged beam to be exactly matched into an ESQ channel.

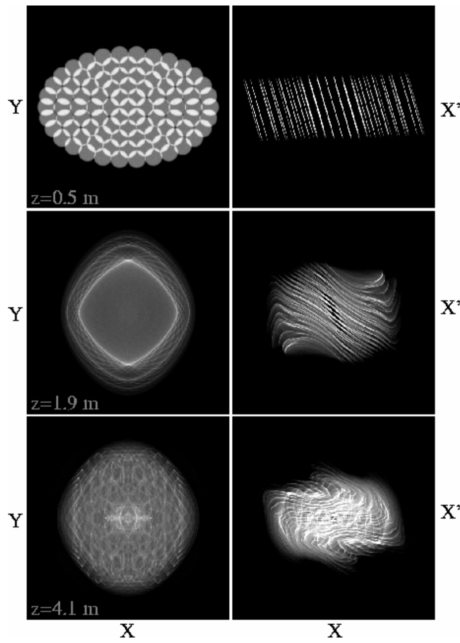

Fig. 5. Multiple (91) beamlets merged in configuration space (left column) and phase space (right column) at various z locations.

An innovative way to match beams into an ESQ channel is to start with an elliptical pattern of beamlets such that the final beam spot is an ellipse with the proper matching envelope divergence. The matching section, as shown in Figure 4, is very short, with minimal beam envelope excursion.

The emittance growth in merging beamlets is minimized when the beamlet energy is high, the number of beamlets is large, and the beamlets are close to each others [9]. Recent computer simulations by Grote [10] further show that the final emittance also depends on the initial beamlet convergence angle (best at around -2 to -4 mrads) and the beam's ion temperature. Nevertheless the ion temperature dependence is weak, and thus ion sources with high ion temperature can be used as long as the average current density remains high. Figure 5 shows the evolution of a

91-beamlet array in configuration space and phase space as produced in simulation. The x and y emittances (4rms) initially rise to different values because of the elliptical shape but later come to an equilibrium value (average between x and y emittance) after a few undepressed betatron periods (about 10 m distance). The beam halo produced by this process is about 1%.

4. Surface Ionization Sources

Until now, the surface ionization source is the type used in almost all HIF experiments. Therefore more detail descriptions on these ion sources are provided here. The surface ionization source is ideal for designing beams with minimum aberration and fast rise time because the emitting surface is a well-defined solid boundary. A large diameter surface ionization source can achieve large current even if the current density is modest. The two main types of surface ionization sources for HIF application are contact ionizers and aluminosilicate sources, both operate at around 1300 deg K. If the beam temperature from a surface ionization source is due only to the thermal temperature of the emitted ions, then these 0.1 eV ions can produce a very bright beam.

4.1 Contact Ionizers

4.1.1 Basic Principles of Contact Ionizers

The definitive work on contact ionization was published by Taylor and Langmuir in 1933 [11]. Contact ionization is due to quantum tunneling of an electron between the metal's Fermi level and an atom's electron cloud. As an atom desorbs from a metal surface, it is more likely to become an ion if the atom's ionization potential is lower than the metal's work function. Thus surface ionization is only effective in generating singly ionized alkali ions such as cesium and potassium. The equilibrium ratio of ion flux (ν_i) to neutral flux (ν_a) departing from the surface is given by the Saha-Langmuir equation:

$$\frac{\nu_i}{\nu_a} = \frac{g_i}{g_a}\exp\left[\frac{e(\phi - I)}{kT}\right] \tag{5}$$

where g_i and g_a are the weighting factors, ϕ is the work function, and I is the ionization potential. For the case of cesium ions emitted from a tungsten surface, ϕ = 4.62 eV, I =3.87 eV, g_i =1 and g_a =2, therefore we find (ν_i/ν_a) = 465 at T = 1273 degree K. Iridium is even better than tungsten because of its higher work function.

An optimum alkali metal coverage on the tungsten surface, typically at the level of a fraction of a monolayer, will lower the tungsten work function, thus enhancing ion emission. For high current, the emitter must be at high temperature to elevate the desorption rate. Unfortunately, according to the above equation, the ratio (ν_i/ν_a) is low when the temperature is high. This means that high current sources will inherently have significant evaporation of neutral atoms. For example at temperature

near 1500 K, the cesium current density can approach 50 mA/cm^2 while the neutral fraction is more than 1%. For most dc applications the neutral atom emission is negligible, but this is an important issue for HIF because an ionizer will continuously evaporate neutrals (at a steady temperature) even though the ion beam duty factor is less than 2×10^{-4}.

4.1.2 Contact Ionizer Construction

A great deal of cesium ionizer technology was developed for early ion propulsion thruster concepts [12]. It was found that sintered porous tungsten can produce large emitters more effectively than solid tungsten. The porous material provides a convenient way to continuously feed alkali metal vapor from the back side to the front side through diffusion. The drawback is that the porous tungsten emits at a lower current density than solid tungsten (at a given temperature) and has a high neutral fraction. Typical porous tungsten material used for ions sources has an 80% solid tungsten density and the tungsten spheres are usually 2–10 microns in diameter [13].

The emitter can be heated either by using heater wire (filament), or by electron bombardment. The most common heater wires are made of tungsten or molybdenum. Heat shields are necessary to minimize radiation heat loss and to keep some components from overheating. In particular, the temperature of the Pierce electrode should be kept low in order to prevent ion emission from the surface of this electrode. Tantalum should be avoided in the heater package because the material is too reactive in case of air or water leaks. Heating up and cooling down of

the surface ionization source should be done slowly (up to an hour for a 17-cm diameter source) to avoid thermal shocks.

The most straight forward way to apply cesium is to use a nozzle to spray cesium vapor from the front side. The nozzle temperature must be above 600 K in order to keep the cesium in the vapor phase. A rear-feed system has a manifold behind the emitter and is connected to a cesium reservoir via a heated tube. Special brazing or e-beam welding is required to join the manifold to the porous tungsten emitter without closing up the pores. In steady state, the emitter is hot and cesium vapor continues to diffuse to the front side. A valve can be used to shut off the cesium vapor flow at the tube but there is no known way to stop cesium that is already in the manifold from diffusing to the front except by cooling down the assembly. A common mode of failure is blockage in the feed tube or pores. This can be a result of contamination turning pure cesium into oxides with higher melting temperatures.

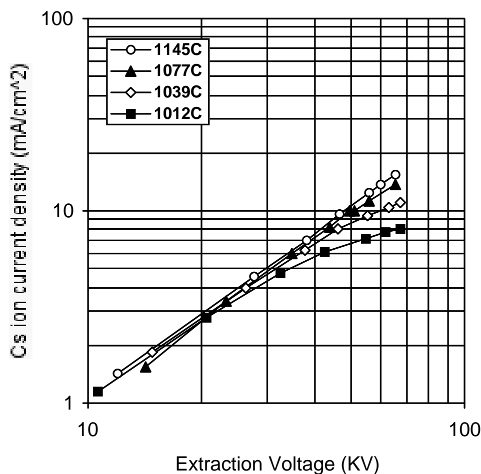

Fig. 6. J-V characteristics for a 2-cm diameter cesium vapor ionizer. Typical pulse length is a few μs, firing at about 0.1 Hz.

One convenient way of loading a surface ionization source with alkali metal for short-duration use is to soak it with an aqueous solution of potassium or cesium carbonate. The carbonate decomposes at about 1000 K releasing carbon dioxide. The alkali metal oxide left on the surface will slowly break down at high temperature to provide alkali metal atoms. Initially the emitting surface will be over-saturated with alkali metal atoms, but since the rate of desorption of neutral atoms from a saturated surface is very high, it takes only a few hours for the doped source to reach steady state operation (with a desirable alkali metal coverage). Normally, such "doped" source is only good for a few days of experiments.

4.1.3 Typical Ionizer Performance in HIF Experiments

Figure 6 shows beam current density as a function of extraction voltage for a diode using a 2 cm diameter cesium vapor ionizer [14]. Typical pulse length was about 3–4 μs at 0.1 Hz. At the highest temperature, the beam current density is space charge limited, therefore the slope of the J-V curve (in log-log plot) is 3/2. At the maximum extraction voltage used, the beam current was 50 mA, corresponding to 15.9 mA/cm^2.

At the lower temperatures with high extraction voltage, the beam current became emission limited. The transition from space charge limit to emission limit was gradual, possibly because not the entire surface became emission limited simultaneously. In order to ensure predictable beam current and therefore fixed beam optics, all HIF injectors that use surface ionization sources are designed to

operate in space charge limited mode. A 30-cm diameter cesium contact ionizer developed for HIF application has produced up to 1 ampere of cesium ion current [15].

4.2 Aluminosilicate Sources

4.2.1 Basic Principles of Aluminosilicate Sources

Aluminosilicate sources are thermionic emitters emitting ions from a hot surface [16,17,18]. Like the electron thermionic emitters, in the absence of electric field the emission current is governed by the Richardson-Dushman equation:

$$J = AT^2 \exp\left[\frac{-e\phi}{kT}\right] \qquad (6)$$

where J is the current density and ϕ is the work function. With strong electric field, the ion emission can be enhanced, mainly due to a reduction in the work function. This phenomenon is known as the Schottky effect in thermionic electron emission. This concept of treating an aluminosilicate source as a thermionic emitter is not exactly correct because the material is not a conductor and the work function is not well defined. Typically when the ion current density is found to scale according to the Richardson-Dushman equation, an empirical work function can be defined to fit the data. As ions are emitted from the surface, the electrical potential will change unless there are ions flowing from underneath the surface to fill in the potential void. Thus the empirical work function is an average quantity, and the variation in work function across the surface may lead to an higher effective ion temperature in comparison to the actual thermal temperature (0.09–0.12 eV) of the emitter.

Assuming the ions are already present at the surface, they can be liberated due to thermal agitation. The ion flow increases if there is an electric field to pull the ions along. Experimental data have shown that the neutral fraction in ion beams generated from aluminosilicate sources is at least an order of magnitude lower than in beams from contact ionizers [19]. The chemical formula for aluminosilicate is $X_2O \cdot Al_2O_3 \cdot n(SiO_2)$, where X is the desired alkali metal element such as Li, Cs or K, and n is an integer determining the type of aluminosilicate crystals. For n = 2, 4 and 10, the corresponding analog natural minerals are β-eucryptite, spodumene and mordenite. The basic crystal structure of this material is silica with some portion of the Si^{4+} ions in the crystal replaced by Al^{3+} ions. Adding a loosely bounded alkali ion compensates the electric charge deficiency produced by this replacement. Since the silica crystalline structure is very open with large tunnels, the alkali ions can move freely making aluminosilicate a good ionic conductor but not an electronic conductor.

4.2.2 Aluminosilicate Source Construction

In some ways, the aluminosilicate source is superior to the contact ionizer because it does not require a metal vapor feed system, does not critically depend on the porosity of the tungsten substrate, and does not evolve a lot of alkali metal vapor. Aside from the possibility of slightly higher ion temperature (due to non-uniform work function), the only major disadvantage of an aluminosilicate source is that the total ion charge delivered during the source’s lifetime is limited due to the limited amount of alkali ions that can be chemically stored in the aluminosilicate

material. Examples of aluminosilicate source usage are in the area of ultra-high vacuum beam collision experiments, ion sputtering, secondary ion mass spectrometer, and plasma diagnostics [20,21]. Aluminosilicate sources are suitable for near-term HIF experiments because of the low duty rate requirements (< few μs per pulse and 0.1 Hz repetition rate).

Fig. 7. A photograph of a 10 cm diameter aluminosilicate emitter with the Pierce electrode.

The construction of an aluminosilicate source is basically the same as an ionizer with an aluminosilicate coating. Commercially available aluminosilicate sources are typically small in diameter (e.g., 1/4 inch) and their coatings are not very uniform. In fabricating large sources, the aluminosilicate coatings often have physical defects such as cracks and fractures, or have difficulty enduring many heat cycles. Recently we have successfully advanced the technique of uniformly coating large sources with diameter up to 10 cm and a spherical emitting surface. The aluminosilicate layer is typically 0.25–0.5 mm thick with no defects [22].

When preparing the aluminosilicate powder, aluminum oxide, silicon dioxide and carbonate of the alkali metal are stoichiometrically mixed according to the type of aluminosilicate required. The mixture is heated in an air furnace to chemically react:

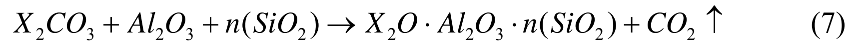

$$X_2CO_3 + Al_2O_3 + n(SiO_2) \rightarrow X_2O \cdot Al_2O_3 \cdot n(SiO_2) + CO_2 \uparrow \qquad (7)$$

After reaction, the aluminosilicate is ground to a fine powder of 100–400 mesh size. By mixing the aluminosilicate powder with a small amount of de-ionized water to form a "mud", one can spread a layer of aluminosilicate with fairly uniform thickness on the substrate. After drying in air, the unit is placed in a vacuum furnace at about 1800 K for sintering. There are some key points to ensure a successful outcome. First of all, the tungsten substrate is etched to open up the pores. Secondly, fine aluminosilicate powder (400 mesh) should be used in this region in order for the aluminosilicate to melt into the pores. This method produces a good interface between the aluminosilicate and the metal substrate, thus preventing future separation after many heat cycles. Similar to the process of firing ceramics, the aluminosilicate mud must be air dried slowly to prevent cracking. Furthermore, we found that it was better to use a mixture of various powder sizes than just using the finest powder because coatings made from the finest powder shrink too much.

4.2.3 Typical Aluminosilicate Source Performance

Figure 8 shows typical I-V curves indicating how the maximum beam current density varies with emitter temperature. At T = 1373 K, a current density of up to 80 mA/cm^2 of K^+ was achieved (pulse length of a few μs and repetition rate of about 0.1 Hz) [19]. The beam current would droop over a long pulse, or if the repetition rate is too high.

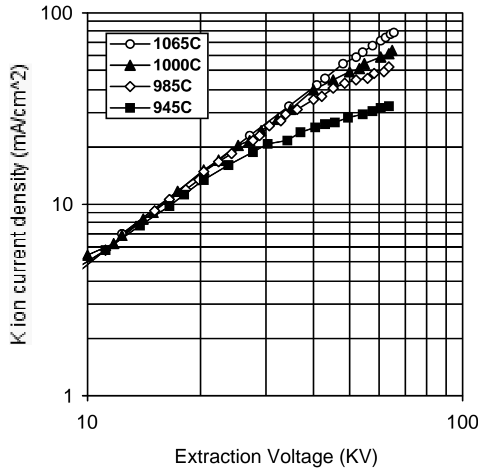

Fig. 8. J-V characteristics of a fully activated potassium aluminosilicate source.

A 17-cm diameter aluminosilicate source was developed for a 2 MeV injector built for the ILSE/Elise project [23]. The injector performance was satisfactory in meeting the specifications of 0.8 A K^+ ion beam with a normalized edge emittance < 1.0 π mm.mrad. Recently the 17-cm source was replaced by a 10-cm source to improve beam optics for the HCX experiment [24,25]. Experimental results were found to have good agreement with computer simulations. A schematic diagram of the injector is shown in Figure 9.

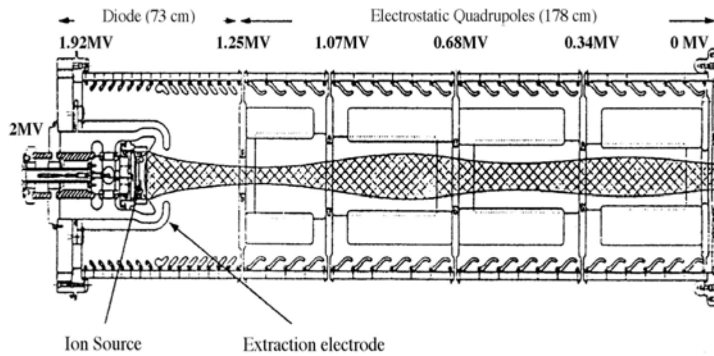

Fig. 9. Schematic diagram of the HCX injector with a large diameter aluminosilicate ion source.

In summary, the surface ionization sources are frequently used in many HIF experiments because they meet the requirements of high current, high brightness, low gas pressure, high reliability, and are generally easy to use. However, this type of ion source has some inherent disadvantages such as the emission of alkali metal vapor into the accelerator, low power efficiency (because the heater is on continuously), limited lifetime, and low average current density for high current beam transport. These are the motivations for us to look for better ways to build ion sources for future HIF drivers even though the surface sources may meet near-term single-beam HIF experimental needs.

5. Metal Vapor Vacuum Arc Sources and Laser Ion Sources

One way of generating plasma is to use a high power density spark discharge. Typical examples are the laser ion sources and the metal vapor vacuum arc (MEVVA) ion sources. The main advantage of these sources is low pressure (no

gas required) while the main disadvantage is mixed ion charge states. In a typical setup, a plasma plume is created by the discharge and the flow is directed towards an extraction grid for beam formation. The velocity distribution of ions in the plume results in ion separation at the end of a long drift distance. Usually ions with higher charge-state acquire more kinetic energy and so they arrive early at the extraction grid. Since the plume also expands transversely, the plasma ions are cooled to a lower transverse ion temperature—an effect that is good for making low emittance beams if the plasma density across the extraction area is still uniform. On the other hand, any unsteadiness of the plasma plume can result in fluctuation of the beam-forming meniscus—an effect that can cause large emittance.

In a MEVVA source, a cathode spot vaporizes the cathode material to produce a plasma plume. Thus the MEVVA source can produce ions of conductive solids. The useful life time of a cathode is about 10^6 shots. For typical arc voltage and current of 1 kV and 500 A, ion current density in the beam extraction area can be in the tens of mA/cm^2 range. Early attempts to use MEVVA sources for HIF [26, 27] found problems related to noise, pulse-to-pulse reproducibility, and mixed charge states. Recently there are improvements in beam uniformities and reduced noise. For example, at GSI, the beam noise was significantly reduced by directing the plasma plume to flow through a pair of biased grids using a guiding magnetic field [28]. A strong magnetic field applied near the cathode was found to enhance the average charge state of ions in the beam. Introducing gas pressure in the chamber and in the beam line also improved the beam quality but at the expense of lowering the average charge state [29].

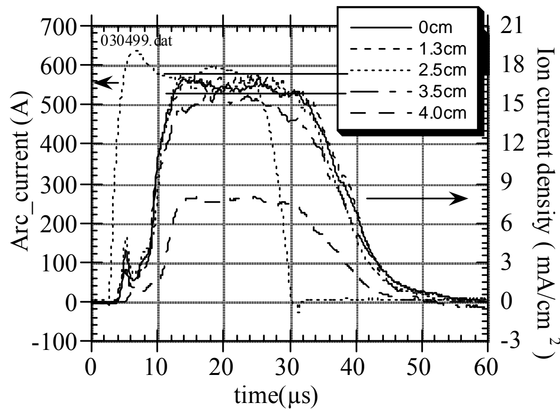

Fig. 10. Current pulses from a MEVVA source taken at various radial positions.

In recent experiments [30, 31], a gadolinium ion beam was produced at a current density of about 20 mA/cm^2 and was uniform to within 2% over a diameter of 60 mm (see Fig. 10). The fluctuations were within 3% rms over a pulse length of 20 μs. Among the various metals (Pb, Y, Gd, Ba) being tested, barium was found to have the best charge state distribution for HIF because it contained more than 95% of 2+ charge state ions. A simple explanation is that the ionization potential from Ba^{++} to Ba^{+++} is 34.45 eV which is many times higher than the 5.54 eV and 10.00 eV for the first 2 levels of ionization. This charge state distribution was obtained when the arc reached steady state at 200 μs after the arc initiation. In general, there were more high charge state ions and impurity ions at the instant when the plume just arrived at the extraction grid and so the charge state distribution was not as pure as that during later time. On a much shorter time scale, strontium (Sr) was found to have a charge state distribution dominated by 2+ at 10 μs after the arrival time [32].

Bismuth is another good candidate for HIF because it is the heaviest non-radioactive metal and it can have a charge state distribution dominated by 1+ (at low arc current). Furthermore, bismuth is isotopically pure and low cost. Recently Anders et al [33] produced a current density of 18 mA/cm^2 using an aperture diameter of 2 mm. The normalized 4-rms emittance was 0.006 π-mm-mrad (measured by the slit-scanner method), corresponding to an equivalent beam temperature of 1.76 eV. Since the beam current and the emittance both increased almost linearly with the arc current, the beam brightness decreased with increasing beam current.

The laser ion source is similar to the MEVVA source in many ways. Both sources produce a plasma plume that expands over a drift region before beam extraction. Even the repetition rates and life-times are similar. At up to 100 J per pulse, the laser ion source can produce very high power density (> 10^{13} W/cm^2) on a target spot, so the average charge state can be higher than that produced by the MEVVA source. Laser ion sources have been used for heavy ion high energy physics accelerators in CERN and TWAC [34,35]. The laser ion source can easily produce a large ion current, but the very wide spread of charge state distribution is a problem for the induction linac approach to HIF. Another obstacle for applying laser ion sources to a HIF driver system is the requirement of multiple-beam geometry; it is not clear if a single laser can be used to drive several targets by doing fast switching. So far, not much work has been done to develop laser ion sources for HIF experiments.

6. Plasma Ion Sources for HIF

While the surface ionization source is ideal for large diameter geometry, the plasma ion source is more suitable for merging a large number of high intensity beamlets to obtain high current. The gas discharge ion source discussed below is the multicusp type. Here we concentrate our discussion on issues related to HIF application.

In merging beamlets into a large beam, the final emittance is dominated by emittance growth in the merging process. Our simulation found that 1–2 eV beam ion temperature was acceptable [10]. If the accelerator grid transparency is less than 20%, then the current density of each beamlet must be near 100 mA/cm^2 in order for the average current density to meet HIF requirements. Another important criterion for HIF ion sources is the level of gas flow. It is important to minimize the gas flow because significant charge exchange can occur in the extraction region below a few hundred keV where the charge exchange cross-section is highest. Charge exchange produces ions at less than full energy and therefore increases the beam's energy dispersion (equivalent to large longitudinal emittance).

The conventional multicusp type plasma source is excellent for producing an array of high current density beamlets. Furthermore, due to the requirement of short beam pulse (less than 20 μs), the discharge can be efficiently produced by using RF power.

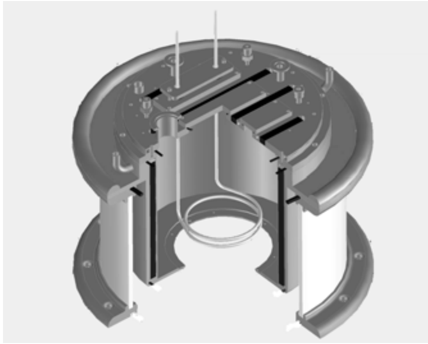

Figure 11. Cutout view of the multicusp source with the embedded RF antenna.

In a series of experiment to characterize the properties of these beamlets, Kwan et al used a 26 cm ID x 25 cm deep chamber driven by a RF antenna at 13 MHz to create argon plasma [36,37,38]. A cut-out view of the ion source is shown in Fig. 11. Typically, the plasma started at least 500 μs before turning on the high voltage extraction pulse. The RF plasma source had good gas efficiency with the argon gas pressure optimized at around 2 mTorr. Figure 12 shows the current density data taken from a 2.5-mm diameter aperture. Up to 100 mA/cm^2 (i.e. 4.9 mA per beamlet) was produced using 80 kV extraction voltage. The normalized 4-rms emittance was 0.0186 π-mm-mrad. From time of flight measurements, the Ar^{2+} and Ar^{3+} fractions was found to increase with RF power. At the power level that produced high current density, the singly-charged fraction was near 90%. The uniformity of current density over a large extraction area (measured by imaging an array of 61 beamlets on a kapton film) was confirmed to be within a few percent.

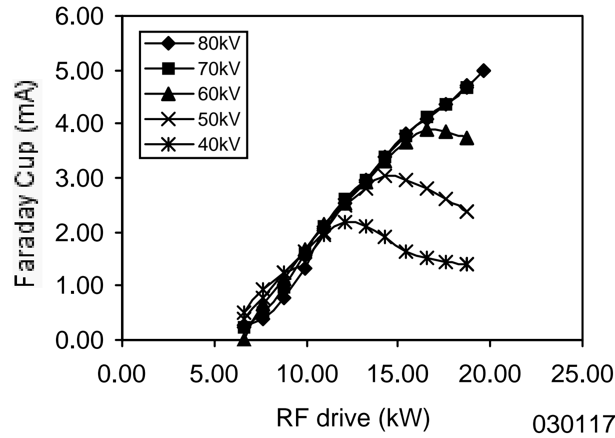

Fig. 12. Argon ion beam current from a 2.5-mm diameter aperture under various extraction voltage.

In the most recent experiment, beamlets were accelerated to 400 kV through a series of electrodes. The maximum voltage gradient on these electrodes exceeded 100 kV/cm, thus provided sufficient focusing to transport the 100 mA/cm^2 beamlets. Figure 13 is a schematic diagram of the accelerator and Fig. 14 shows a photograph of an electrode with the 61-aperture array. It is interesting to note that the voltages applied to the electrodes were not monotonically decreasing in order to create the Enizel lens focusing effect. Further details of the results in this experiment and a subsequent experiment that converge the beamlets into an electrostatic (ESQ) channel will be reported in a separate article.

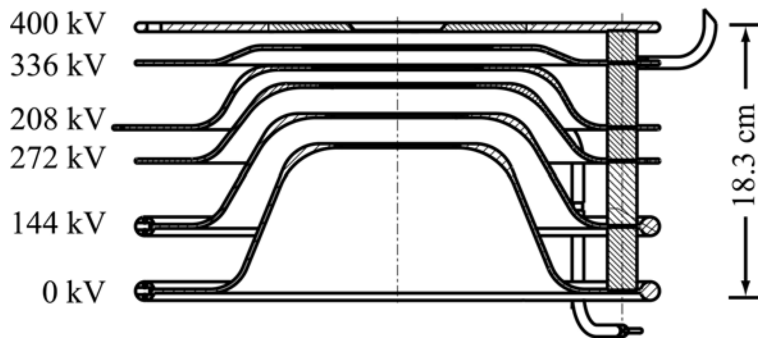

Fig. 13. Schematic diagram of the full-gradient accelerator.

Fig. 14. Photograph of an electrode in the full-gradient accelerator showing the 61-beamlet aperture array.

7. Negative Ion Sources for HIF

As long as an ion beam can deliver pulsed power to a target, it can consist of either positive or negative ions. However, negative ion beams have two advantages. First, for very high current beams, the beam potential can exceed several kV. Such large positive beam potential traps electrons (from beam ionizing the background gas and secondary electrons from the beam pipe), leading to instability and

emittance growth. This “electron cloud” problem can be avoided by using negative ion beams to repel electrons.

Another characteristic of negative ions is that they can be easily converted into neutral atoms. An intense neutral particle beam has no space charge and can be focused down to a small spot. Of course, a significant level of background gas in the target chamber can strip electrons from the beam ions and therefore turn them into high charge state positive ions. Nevertheless, computer simulations have shown that a negative ion beam may attain a smaller spot size than a comparable positive ion beam.

The halogen negative ions was proposed by Grisham [39,40] for HIF because the halogen atoms have high electron affinities, at around 3 to 3.6 eV. The negative ions can be converted into neutrals via laser photo-detachment. Recent experiments with chlorine (it was chosen because the substance is in the gas phase at room temperature) have demonstrated a negative chlorine ion current density of 45 mA/cm^2. The negative ions were 99.5% pure atomic Cl^-, and the electron-to-Cl^- ratio was as low as 7:1 [41]. Such small ratio of electron/Cl^- suggested that the negative ion density was nearly equal to the positive ion density in the plasma. Further experiments are in progress to measure the beam emittance.

8. Conclusion

For heavy ion beam driven inertial fusion, the ion sources must produce beams of heavy ions with very high current and high brightness. However, fundamental beam transport physics limits the simultaneous attainment of high

current and high brightness. Brightness can be achieved by using either high current density or low emittance, or a combination of both. When beamlets are merged together to form a high current beam, the current density of each beamlet must be very high in order to compensate for the loss of brightness due to emittance growth.

In the traditional approach, a large area surface ionization source is used to produce a high current beam (per channel) at relatively low current density. Even with a large diameter the emittance can still be low because the ion temperature is low for surface ionization sources. A recent approach is to merge an array of beamlets, such that with sufficiently high beamlet current density and grid transparency, the average current density can be adequate. This approach allows many ion source options, and is not limited to surface ionization sources. In this paper, we have discussed contact ionization sources, aluminosilicate sources, metal vapor vacuum arc sources, gas plasma sources, and negative ion sources for HIF. We are continuing to seek improvement on these ion sources in order to meet the challenging and sometimes evolving HIF requirements.

References

[1] D.A. Callahan-Miller, M. Tabak, Nuclear Fusion **39**, 1547 (1999).

[2] R.O. Bangerter, in *Proc. of Inter. Symp. on Heavy Ion Inertial Fusion, Frascati, Italy*, 25-28 May, 1993, Nuovo Cimento **106A**, N.11, 1445, (1993).

[3] J.R. Pierce, in *Theory and Design of Electron Beams*, (Van Nestrand, New York, 1954), p16.

[4] L.L. Alston, in *High Voltage Technology* (Oxford Univ. Press, New York, 1968), p.65.

[5] L. Cranberg, J. Appl. Phys. **23**, 518 (1952).

[6] E.P. Lee, R.O. Bangerter, C.F. Chan, A. Faltens, J. Kwan, E. Henestroza, K. Hahn, P. Seidl, J.J. Barnard, A. Friedman, D.P. Grote, W.M. Sharp, in *Proc. of Inter. Symp. on Heavy Ion Inertial*

Fusion, Princeton, New Jersey, Sept. 6-9, 1995; in Fusion Engineering and Design, **32-33**, 323, (1996).

[7] J.W. Kwan, O.A. Anderson, D.N. Beck, F.M. Bieniosek, C.F. Chan, A. Faltens, E. Henestroza, S.A. MacLaren, P.A. Seidl, L. Ahle, D.P. Grote, E. Halaxa, C.T. Sangster, and W.B. Herrmannsfeldt, in *Proceedings of the Particle Accelerator Conference, New York City, New York,* (Mar 28, 1999), p. 1937.

[8] J.W. Kwan, L. Ahle, D.N. Beck, F.M. Bieniosek, A. Faltens, D.P. Grote, E. Halaxa, E. Henestroza, W.B. Herrmannsfeldt, V. Karpenko, and T.C. Sangster, Nucl. Instrum. Meth. Phys. Res. **A 464**, 379 (2001).

[9] O.A. Anderson, *Proc. of Inter. Symp. on Heavy Ion Inertial Fusion;* Fusion Engineering and Design, **32-33**, 209 (1996).

[10] D.P. Grote, E. Henestroza, J.W. Kwan, Phy. Rev. Special Topics-Accel. & Beams **6**, 014202 (2003). http://prst-ab.aps.org/

[11] J.B. Taylor and I. Langmuir, Phys. Rev. **44**, 432 (1933).

[12] G.R. Brewer, in *Ion Propulsion*, (Gordon and Breach, New York, 1970), p. 112.

[13] A.T. Forrester, in *Large Ion Beams,* (Wiley, New York, 1988), p236.

[14] J.W. Kwan, W.W. Chupp, and S. Eylon, Proc. Particle Accelerator Conf., p2755, Vancouver, March, (1997).

[15] S. Abbott, W. Chupp, A. Faltens, W. Herrmannsfeldt, E. Hoyer, D. Keefe, C.H. Kim, IEEE Trans. Nucl. Sci. **26**, 3095 (1979).

[16] J.L. Hundley, Phys. Rev. **30**, 864 (1927).

[17] J.P. Blewett and E.J. Jones, Phy. Rev. **50**, 464 (1936).

[18] R.K. Feeney, W.E. Sayle, II, and J.W. Hooper, Rev. Sci. Instrum. **47**, 964 (1976).

[19] E. Chacon-Golcher, D. Baca, J.W. Kwan, Rev. Sci. Instrum. **73**, 1036 (2002).

[20] S.I. Kim and M. Seidl, J. Appl. Phys. **67**, 2704 (1990).

[21] A.E. Souzis, W.E. Carr, S.I. Kim and M. Seidl, Rev. Sci. Instrum. **61**, 788 (1990).

[22] D. Baca, E. Chacon-Golcher, J. W. Kwan, J. K. Wu, in *Proc. Particle Accelerator Conference, Portland, Oregon*, May 12-16, (2003).

[23] S.S. Yu, S. Eylon, E. Henestroza, C. Peters, L. Reginato, A. Tauschwitz, D. Grote, F. Deadrick, in *Proc. Inter. Symp. on Heavy Ion Inertial Fusion, Princeton, New Jersey, Sept. 6-9, 1995*; in Fusion Engineering and Design **32-33**, 309 (1996).

[24] J. W. Kwan, F. M. Bieniosek, E. Henestroza, L. Prost and P. Seidl, Laser and Particle Beams **20**, 441 (2002).

[25] F. M. Bieniosek, C. M. Celata, E. Henestroza, J.W. Kwan, L. Prost, P. A. Seidl, A. Friedman, D. P. Grote, S. M. Lund, and I. Haber, Phys. Rev. Special Topics-Accelerators and Beams, **8**, 010101 (2005)

[26] S. Humphries, Jr., C. Burkhart, and L.K. Len, in *The Physics and Technology of Ion Sources*, edited by I.G. Brown, (Wiley, New York, 1989), p. 397-419.

[27] S. Humphries, Jr., H. Rutkowski, J. Appl. Phys. **67**, 3223 (1990).

[28] E.M. Oks, P. Spaedtke, H. Emig, and B.H. Wolf, Rev. Sci. Instrum. **65**, 3109 (1994).

[29] H. Reich, P. Spaedtke, and E.M. Oks, Rev. Sci. Instrum. **71**, 707 (2000).

[30] F. Liu, N. Qi, S. Gensler, R.R. Prasad, M. Krishnan, and I.G. Brown, Rev. Sci. Instrum. **69**, 819 (1998).

[31] N. Qi, J. Shein, R.R. Prasad, M. Krishnan, A. Anders, J.W. Kwan, and I.G. Brown, Nucl. Instrum. Meth. Phys. Res. **A 464**, 576 (2001)

[32] A. Anders and J.W. Kwan, Nucl. Instrum. Meth. Phys. Research **A 464**, 569 (2001).

[33] A. Anders and E. Chacon-Golcher, J. Appl. Phys. **93**, 2298 (2003).

[34] B. Yu. Sharkov, A.V. Shumshurov, V.P. Dubenkow, O.B. Shamaev, and A.A. Golubev, Rev. Sci. Instrum. **63**, 2841 (1992).

[35] B. Yu. Sharkov, S. Kondrashev, I. Roudskoy, S. Savin, A. Shumshurov, H. Haseroth, H. Kugler, K. Langbein, N. Lisi, H. Magnusson, R. Scrivens, J.C. Schnuringer, J. Tambini, S. Homenko, K. Makarov, V. Roerich, A. Stepanov, and Yu. Satov, Rev. Sci. Instrum. **69**, 1035 (1998).

[36] J. W. Kwan, D. P. Grote, and G. A. Westenskow, Rev. Sci. Instrum. **75**, 1838 (2004).

[37] G. Westenskow.; Grote, D.; Hall, R.; Kapica, J.; Kwan, J.; Waldron, W., "High Current Ion Source Development for Heavy Ion Fusion," The Third Inter. Conf. on Inertial Fusion Sciences and Applications (IFSA), Monterey, CA, Sept. 2003, p702.

[38] L. Ahle, R.P. Hall, and A.W. Molvik, J.W. Kwan, and K.N. Leung, Rev. Sci. Instrum. **73**, 1039 (2002)

[39] L.R. Grisham, Nucl. Instrum. Meth. **A 464**, 315 (2001).

[40] L.R. Grisham, Fusion Sci. & Tech. **43**, 191, (2003).

[41] S.K. Hahto, S.T. Hahto, J.W. Kwan, K.N. Leung, and L.R. Grisham, Rev. Sci. Instrum. **74**, 2987 (2003).